NODAL in the Uterus Is Necessary for Proper Placental Development and Maintenance of Pregnancy 1

Authors: Park, Craig B., DeMayo, Francesco J., Lydon, John P., and Dufort, Daniel

Source: Biology of Reproduction, 86(6)

Published By: Society for the Study of Reproduction

URL: https://doi.org/10.1095/biolreprod.111.098277

BIOLOGY OF REPRODUCTION (2012) **86**(6):194, 1–13
Published online before print 29 February 2012.
DOI 10.1095/biolreprod.111.098277

NODAL in the Uterus Is Necessary for Proper Placental Development and Maintenance of Pregnancy[1]

Craig B. Park,[3,4] Francesco J. DeMayo,[6] John P. Lydon,[6] and Daniel Dufort[2,3,4,5]

[3]*Division of Experimental Medicine, Royal Victoria Hospital, McGill University Health Centre, Montreal, Quebec, Canada*
[4]*Centre for the Study of Reproduction at McGill, Royal Victoria Hospital, McGill University Health Centre, Montreal, Quebec, Canada*
[5]*Department of Obstetrics and Gynecology, Royal Victoria Hospital, McGill University Health Centre, Montreal, Quebec, Canada*
[6]*Department of Molecular and Cellular Biology, Baylor College of Medicine, Houston, Texas*

ABSTRACT

Preterm birth is the single leading cause of perinatal mortality in developed countries, affecting approximately 12% of pregnancies and accounting for 75% of neonatal loss in the United States. Despite the prevalence and severity of premature delivery, the causes and mechanisms that underlie spontaneous and idiopathic preterm birth remain unknown. Our inability to elucidate these fundamental causes has been attributed to a poor understanding of the signaling pathways associated with the premature induction of parturition and a lack of suitable animal models available for preterm birth research. In this study, we describe the generation and analysis of a novel conditional knockout of the transforming growth factor beta (TGFB) superfamily member, *Nodal*, from the maternal reproductive tract of mice. Strikingly, uterine *Nodal* knockout females exhibited a severe malformation of the maternal decidua basalis during placentation, leading to significant intrauterine growth restriction, and ultimately preterm birth and fetal loss on Day 17.5 of gestation. Using several approaches, we characterized aberrant placental development and demonstrated that reduced proliferation combined with increased apoptosis resulted in a diminished decidua basalis and compromised maternal-fetal interface. Last, we evaluated various components of the established parturition cascade and determined that preterm birth derived from the maternal *Nodal* knockout occurs prior to PTGS2 (COX-2) upregulation at the placental interface. Taken together, the results presented in this study highlight an in vivo role for maternal NODAL during placentation, present an interesting link between disrupted decidua basalis formation and premature parturition, and describe a potentially valuable model toward elucidating the complex processes that underlie preterm birth.

NODAL, placenta, preterm birth, transforming growth factor beta, uterus

INTRODUCTION

Successful mammalian reproduction culminates with the induction of parturition and delivery of the fully developed fetus. Term delivery ensures adequate time for embryonic growth and development of the biological systems required for the neonate to survive outside of the nurturing maternal environment. As a result, preterm delivery of immature offspring is a serious complication of pregnancy and is the leading cause of perinatal mortality in developed countries, accounting for approximately 75% of all neonatal deaths [1–3]. Furthermore, premature babies that survive are at an increased risk of developing neurodegenerative disorders, such as cerebral palsy, learning disabilities, impaired vision, or issues associated with psychological development, including behavioral or emotional problems [4, 5]. In addition to the long-term health and social consequences associated with preterm birth, the monetary impact on developed societies is substantial when one considers the services required to assist those who develop disabilities. It is estimated that preterm birth costs the health care system a minimum of $26.2 billion annually in the United States alone [6].

NODAL, a morphogen in the transforming growth factor beta (TGFB) superfamily, plays critical roles during embryonic development by inducing mesoderm formation and patterning the left-right axis [7, 8]. Like other members of the TGFB superfamily, signaling is achieved when diffusible NODAL ligand binds to a cell surface complex comprising type I (ALK4/ALK7) and type II (ActRIIA/ActRIIB) serine/threonine kinase receptors and an EGF-CFC coreceptor (cripto/cryptic). Activation of the receptor complex results in the downstream phosphorylation of SMAD2/3 and subsequent binding of SMAD4 prior to nuclear translocation and regulation of gene expression. NODAL signaling is regulated by complex autoregulatory interactions that propagate and restrict activity as NODAL binding results in the production of more NODAL ligand and its diffusible inhibitor, Lefty (for detailed reviews see Shen [9] and Schier [10]). Although NODAL is best known for its roles during mammalian development, components of the NODAL signaling pathway have also been implicated in many events associated with mammalian reproduction [11]. Recently, our laboratory [12] and others [13] have been characterizing the expression pattern and potential roles of NODAL signaling in the adult uterus of mice and humans, respectively. Interestingly, NODAL is expressed throughout the mouse uterus during early pregnancy and generates a banding pattern along the proximal-distal axis of the uterine horn at the time of implantation that directly correlates with the

[1]Supported by grant MOP-82780 from the Canadian Institutes of Health Research (CIHR) to D.D. C.B.P. is supported by awards from the MUHC-RI and CIHR and is a member of the CIHR-REDIH program.
[2]Correspondence: Daniel Dufort, Royal Victoria Hospital, 687 Pine Ave. West, Room F3-24, Montreal, QC H3A 1A1, Canada.
E-mail: daniel.dufort@mcgill.ca

Received: 6 December 2011.
First decision: 5 January 2012.
Accepted: 16 February 2012.

eISSN: 1529-7268 http://www.biolreprod.org
ISSN: 0006-3363

interimplantation nodes. Furthermore, NODAL from a uterine source contributes to the maternal-fetal interface of the conceptus, ultimately becoming restricted to a thin layer of the placental decidua parietalis during the later stages of pregnancy [12].

In order to further investigate the potential roles of NODAL signaling during mammalian reproduction, we report here the generation of a tissue-specific conditional knockout of *Nodal* in the mouse maternal reproductive tract. In addition to highlighting potential roles during early pregnancy, uterine *Nodal* deletion promotes preterm birth and fetal loss by disrupting the maternal-fetal interface during placentation. Despite the prevalence and severity of preterm birth, our current understanding of parturition remains relatively unclear [3]. Moreover, the most significant impediment in our efforts to decrease the occurrence of premature birth has been directly attributed to our lack of understanding of the signal transduction pathways that are associated with premature parturition [14]. This is compounded by a lack of suitable animal models available for preterm birth research [15]. The results presented in this study advance our knowledge of parturition by 1) providing evidence that the NODAL signaling pathway is required to ensure successful delivery at term and 2) presenting an interesting link between disrupted placentation and preterm birth.

MATERIALS AND METHODS

Generation of Uterine Nodal$^{\Delta/\Delta}$ *Mice*

All animal care and experimental procedures were approved by the Animal Care Committee of the Royal Victoria Hospital and were in accordance with the regulations established by the Canadian Council on Animal Care. Mice with loxP sites flanking exons 2 and 3 of the *Nodal* gene ($Nodal^{loxP/loxP}$) on a mixed background were previously generated and kindly donated by E. J. Robertson (University of Oxford) [16]. Progesterone receptor (*Pgr*)-Cre mice ($Pgr^{Cre/+}$) on a C57BL6/129 background were generously provided by F. J. DeMayo and J. P. Lydon (Baylor College of Medicine) [17]. Both strains have previously been reported to demonstrate normal fertility, and $Pgr^{Cre/+}$ mice have been used in numerous studies to investigate uterine-specific gene function [18, 19]. $Nodal^{loxP/loxP}$ and Pgr^{Cre} strains were crossed, and the offspring were genotyped by tail snip digestion and PCR. The $Nodal^{loxP}$ (290 bp) and $Nodal^{+}$ (220 bp) alleles were amplified by touchdown PCR (94°C, 58°C*, 72°C [30 sec] for seven cycles *decreasing 0.5°C per cycle; 30 cycles at 94°C, 55°C, 72°C [30 sec]; 5′-ATTCCAGCAGTTGAGGCAGA-3′; 5′-GCTATGCCACG CAGAACC-3′), and the Pgr^{Cre} (550 bp) and Pgr^{+} (300 bp) alleles were amplified by standard PCR (94°C, 60°C [1 min each], 72°C [2 min] for 30 cycles; 5′-ATGTTTAGCTGGCCCAATG-3′; 5′-TATACCGATCTCCCTG GACG-3′; 5′-CCCAAAGAGACACCAGGAAG-3′). Double heterozygotes ($Nodal^{loxP/+}$, $Pgr^{Cre/+}$) were crossed with $Nodal^{loxP/+}$, $Pgr^{+/+}$ mice to acquire the first generation of the tissue-specific, conditional knockout strain (henceforth $Nodal^{\Delta/\Delta}$) and double-heterozygous controls ($Nodal^{\Delta/+}$). Tissue-specific Cre-mediated *Nodal* deletion was verified by genomic PCR (data not shown), Western blot analysis, and immunofluorescence (described below). Strain lineage was maintained by breeding double heterozygotes with age-matched floxed mice that did not inherit the *Pgr-Cre* allele ($Nodal^{loxP/loxP}$, $Pgr^{+/+}$).

Mating, Manipulation, and Monitoring of Transgenic Mice

Transgenic females were mated with CD1 males, and the day of vaginal plug visualization was assigned as Day 0.5 postcoitum. 1) Females used to assess postimplantation whole-mount decidualization were killed on Day 8.5 postcoitum, and the uterus was dissected in PBS. Decidua swellings were counted, and the individual conceptus sites were isolated, blotted dry, and weighed. 2) Females used to quantify intrauterine growth restriction (IUGR) were culled on Days 10.5, 12.5, 15.5, and 16.5 postcoitum, and fetuses were dissected in PBS, dried, and weighed. Photographs of the whole-mount uteri and Day 15.5/16.5 fetuses depicting relative size were taken in the same photographic frame on a Fotodyne illuminated platform with a Canon Powershot SD1300 digital camera. 3) Females monitored to assess parturition were observed daily (morning to late afternoon) from Day 15.5 until birth. Preterm birth was defined as the induction of parturition prior to Day 19.5, and fetal loss was defined as stillborn or death of the pup within 24 h of birth.

Tissue Histology

Whole uteri (Days 6.5–10.5), dissected placentae (Day 12.5), or ovaries were dissected in PBS and fixed overnight at 4°C in 4% paraformaldehyde (PFA)/PBS. Samples were dehydrated with 100% ethanol (2×, 30 min each), treated with xylenes:ethanol (1:1; 1×, 30 min), and submersed in xylenes (2×, 1 h each). The tissue was placed in melted paraffin wax (Tissue Tek) and xylenes (1:1) for 1 h at 60°C, followed by pure paraffin overnight under a vacuum. Samples were embedded at room temperature and the blocks were solidified at −20°C. Seven-micrometer sections were cut with a Leica RM2145 microtome and dried overnight. Slides were then washed in xylenes, rehydrated with a decreasing ethanol gradient (100%, 95%, 85%, 75%, 50%, 20%; 2 min each), and counterstained with Nuclear Fast Red (Sigma) or hematoxylin & eosin (Surgipath). The stained sections were dehydrated with increasing ethanol concentrations, cleared in xylenes, and mounted with paramount glue.

Immunohistochemistry

Day 10.5 paraffin-embedded uterine sections were rehydrated as described above, treated with 3% hydrogen peroxide in methanol (20 min), boiled in 10 mM sodium citrate, pH 6.0 (15 min), and allowed to cool at room temperature. Slides were then washed with 0.5% Triton X, 0.2% bovine serum albumin/PBS (2×, 5 min), and blocked with 1.35% heat-inactivated goat serum diluted in wash buffer for 30 min at 37°C within a humidified chamber. The samples were then rinsed with 0.1% Tween 20/PBS (3×, 5 min) and incubated overnight at 4°C with 1:100 rabbit anti-proliferating cell nuclear antigen (anti-PCNA; sc-7907; 0.2 mg/ml; Santa Cruz Biotechnology) or goat anti-MKI67 (sc-7846; 0.2 mg/ml; Santa Cruz Biotechnology) diluted in 1% bovine serum albumin/PBS. Slides were then rinsed, probed with 1:500 goat anti-rabbit horseradish peroxidase (HRP; sc-2004; 0.4 mg/ml; Santa Cruz Biotechnology) or donkey anti-goat HRP (sc-2020; 0.4 mg/ml; Santa Cruz Biotechnology) for 1 h at room temperature, and visualized using a 3,3′-diaminobenzidine kit (Sigma). Uterine sections were counterstained with hematoxylin, dehydrated, cleared in xylenes, and mounted with paramount glue. All tissue section-based experiments (immunohistochemistry, in situ hybridization, etc.) used at least three placentae per category.

Cyroembedding and Immunofluorescence

Uteri and placentae used for immunofluorescence or in situ hybridization were dissected in cold PBS and fixed overnight at 4°C in 4% PFA/PBS. Uteri were treated with 15% sucrose for 3 h and 25% sucrose overnight at 4°C before embedding in Shandon Cyromatrix (Thermo Scientific) at −80°C. Ten-micrometer sections were cut with a cryotome, mounted on Super Frost Plus slides (VWR), and stored at −80°C. Immunofluorescence was performed as previously described [12]. Slides were probed with rabbit anti-NODAL (sc-28913; 0.2 mg/ml; Santa Cruz Biotechnology) diluted 1:100 and were detected with 1:500 Alexa-488 goat anti-rabbit (AC11008; 1 mg/ml; Invitrogen) antibody. Sections were counterstained with propidium iodide (0.2 μg/ml) and mounted in Mowiol 4–88 (Calbiochem). Uteri sections were analyzed with the Zeiss LSM 510 Meta confocal microscope and associated software.

In Situ Hybridization

All full-length cDNA used to generate the hybridization probes were kindly provided by J. Cross (University of Calgary). Tissue samples were cyroembedded, sectioned, and stored as described above. In situ hybridization was performed with the aid of the J. Cross Laboratory using the protocol developed and detailed in Simmons et al. [20]. Briefly, slides were rehydrated in PBS, postfixed with 4% PFA/PBS (10 min, 4°C), and treated with proteinase K (30 μg/ml; 12 min; Roche). Sections were acetylated (0.25% acetic anhydride; 10 min) and hybridized with digoxigenin (DIG)-labeled probes overnight at 65°C. DIG-labeled probes were generated following the manufacturer's protocol (Roche) and were used at a concentration of 1:2000 with a 1-μg starting template DNA. Following washes in SSC (150 mM sodium chloride, 15 mM sodium citrate)/50% formalin/0.1% Tween 20 (2×) and MABT (100 mM maleic acid, 150 mM sodium chloride, and 0.1% Tween 20; 2×), slides were treated with RNase A (20 μg/ml, 30 min), blocked (2% Blocking Reagent [Roche], 20% heat-inactivated goat serum in MABT), and incubated overnight at 4°C with anti-DIG antibody diluted 1:2500 in block solution. Following MABT washes (4×), the sections were rinsed in NTMT

(100 mM NaCl; 100 mM Tris, pH 9.5; 50 mM MgCl; and 0.1% Tween 20) and developed using an NBT/BCIP kit (Promega). Developed sections were counterstained in Nuclear Fast Red, dehydrated with an ethanol gradient, and mounted in Mowiol 4–88.

Western Blot Analysis

Indicated tissue samples (0.5 g) were isolated, rinsed in PBS, and homogenized in extraction buffer (50 mM Tris-HCl, pH 7.2; 10 mM dithiothreitol; 1% Nonidet P-40; 1 mM $CaCl_2$; 5 mM $MgCl_2$; 100 U/ml DNase I; 50 μg/ml RNase A; and 75 μg/ml protease inhibitor cocktail [P2714; Sigma]). Homogenate was centrifuged (10 000 rpm, 10 min, 4°C), and supernatant was resolved on a 12% SDS-PAGE gel. Protein was transferred to polyvinylidene fluoride membrane membrane (GE Healthcare), blocked with 5% skim milk, and probed with rabbit anti-NODAL or rabbit anti-PTGS2 (COX-2; 160106; 0.1 mg/ml; Cayman Chemical) antibodies diluted 1:500 in block solution. Protein was detected with anti-rabbit HRP diluted 1:4000 and the ECL Plus kit (GE Healthcare). Membranes were subsequently stripped, probed with anti-α-tubulin loading control antibody, and developed. Relative protein concentrations were obtained with the Image J quantification software (National Institutes of Health).

TUNEL Assay

Apoptosis was assessed directly on paraffin-embedded sections of Day 10.5 placental tissue with the in situ cell death assay kit (Roche) following the manufacturer's protocol. Sections were pretreated using the proteinase K option (30 μg/ml in 10 mM Tris-HCl, pH 7.5; 20 min), and positive controls were generated by incubation with 2000 U/ml DNase I for 10 min.

Progesterone Quantification

Progesterone concentration in maternal blood serum was quantified by radioimmunoassay with the aid of the B. Murphy laboratory (Université de Montréal; as described in Duggavathi et al. [21]).

Statistics

Figure data are presented as mean ± SEM of independent samples. Statistical analysis comparing two groups was performed using the standard Student two-sided *t*-test. Calculations were confirmed using the GraphPad software. *P* values less than 0.05 were considered statistically significant.

RESULTS

Nodal *Is Efficiently Deleted in the Uteri of* Nodal$^{\Delta/\Delta}$ *Female Mice*

Mice in which the *Nodal* gene is conditionally deleted in the reproductive tract of adult females were generated by mating the floxed *Nodal* (*Nodal*$^{loxP/loxP}$) and *Pgr*-Cre (*Pgr*$^{Cre/+}$) mouse strains (detailed in *Materials and Methods*) [16, 17]. In order to verify the targeted deletion of *Nodal* in the newly generated *Nodal*$^{loxP/loxP}$, *Pgr*$^{Cre/+}$ mouse strain (denoted *Nodal*$^{\Delta/\Delta}$), genomic DNA isolated from adult uterine tissue was confirmed to have complete excision of the floxed sequence, whereas several untargeted tissues (i.e., kidney, lung, tail snip) contained the full-length *Nodal* gene (data not shown). Previous studies of *Nodal* expression conducted in our laboratory have demonstrated that *Nodal* is not present in the uterus prior to coitus; however, robust *Nodal* expression and protein localization was observed in the uterine glandular epithelium during the early peri-implantation period (Days 0.5–3.5 postcoitum) [12]. Although NODAL protein was easily detectable by Western blotting of uterine tissue isolated from double-heterozygous control mice (*Nodal*$^{\Delta/+}$) on Day 3.5, only an extremely faint band was observed in the experimental *Nodal*$^{\Delta/\Delta}$ uteri (Fig. 1a). Furthermore, immunofluorescence did not detect NODAL protein around the glandular epithelium of Day 3.5 *Nodal*$^{\Delta/\Delta}$ uteri that were confirmed to be pregnant by embryo flushing of the contralateral uterine horn (Fig. 1, b–g). Taken together, these results verify that NODAL protein production has been effectively eliminated from the uteri of adult *Nodal*$^{\Delta/\Delta}$ females.

Nodal$^{\Delta/\Delta}$ *Females Exhibit a Reduced Rate of Fertility*

In order to assess the reproductive capabilities of *Nodal*$^{\Delta/\Delta}$ mice, adult females were mated with CD1 males overnight, and successful copulation was determined by the presence of a vaginal plug the following morning (Day 0.5). Interestingly, plugged *Nodal*$^{\Delta/\Delta}$ females demonstrated a reduced ability to establish pregnancy, because mice examined after implantation (on or after Day 5.5) rarely contained decidua swellings or developing embryos (26.3%; n = 19; Fig. 2a and Supplemental Table S1 [all supplemental materials are available online at www.biolreprod.org]). Preliminary analysis suggests this reduced fertility occurs during early reproduction but is not due to a defect in ovulation, because the number of corporal lutea remains unaffected in floxed control (*Nodal*$^{loxP/loxP}$, *Pgr*$^{+/+}$), double-heterozygous control (*Nodal*$^{\Delta/+}$), and *Nodal*-deleted females (*Nodal*$^{\Delta/\Delta}$; data not shown). The precise role of uterine NODAL in facilitating early reproduction is currently under investigation but beyond the primary focus of this study.

Nodal$^{\Delta/\Delta}$ *Females Experience Preterm Birth and Fetal Loss*

Strikingly, pregnant *Nodal*$^{\Delta/\Delta}$ females that overcome the reduced fertility associated with early reproduction ultimately experienced spontaneous preterm birth on Day 17.5 of gestation, a phenotype very rarely observed in mice [15]. A total of 14 pregnant *Nodal*$^{\Delta/\Delta}$ mice were monitored several times daily (0900–2000 h) from Day 15.5 postcoitum until delivery. A total of 9 of the 14 *Nodal*$^{\Delta/\Delta}$ females gave birth prematurely on Day 17.5, 2 days prior to normal term gestation of 19.5 days (Table 1). Two additional *Nodal*$^{\Delta/\Delta}$ females gave birth moderately preterm on Day 18.5, with the remaining pregnancies going to term (11 of 14 preterm; Fig. 2b). Conversely, 17 of 18 pregnant *Nodal*$^{\Delta/+}$ control females gave birth on Day 19.5, with a single premature delivery observed on Day 18.5 (1 of 18 preterm). As a result, pregnant *Nodal*$^{\Delta/\Delta}$ mice experienced spontaneous preterm birth at a significantly higher rate compared with the double-heterozygous females. Despite the early delivery, we did not observe any occurrence of dystocia (abnormally long, difficult delivery) in the experimental *Nodal*$^{\Delta/\Delta}$ females.

In addition to premature parturition, most offspring delivered by *Nodal*$^{\Delta/\Delta}$ females were stillborn or died shortly after birth. Whereas *Nodal*$^{\Delta/+}$ control females averaged 5.4 live and 1.0 dead pups per dam, the experimental *Nodal*$^{\Delta/\Delta}$ mice produced 2.2 live and 3.8 dead pups per dam (Fig. 2c and Table 1). It is important to note, however, most of the live pups obtained from the experimental *Nodal*$^{\Delta/\Delta}$ group were contributed by females that experienced moderately premature (Day 18.5) or term deliveries. Taken together, this suggests the fetal loss is primarily due to premature birth, because pups born to pregnant *Nodal*$^{\Delta/\Delta}$ females that successfully reached term had a greater likelihood of survival.

Whole-Mount Decidualization Appears Normal During Midgestation in Pregnant Nodal$^{\Delta/\Delta}$ Mice

In order to investigate the underlying source of preterm birth and fetal loss in *Nodal*$^{\Delta/\Delta}$ females, whole-mount uteri from pregnant mice were first isolated throughout midpregnancy (Days 6.5–12.5), and the conceptus site number, size, and weight were assessed on Day 8.5. In general, there were no observable differences between whole-mount uteri isolated from the experimental *Nodal*$^{\Delta/\Delta}$ or *Nodal*$^{\Delta/+}$ control females

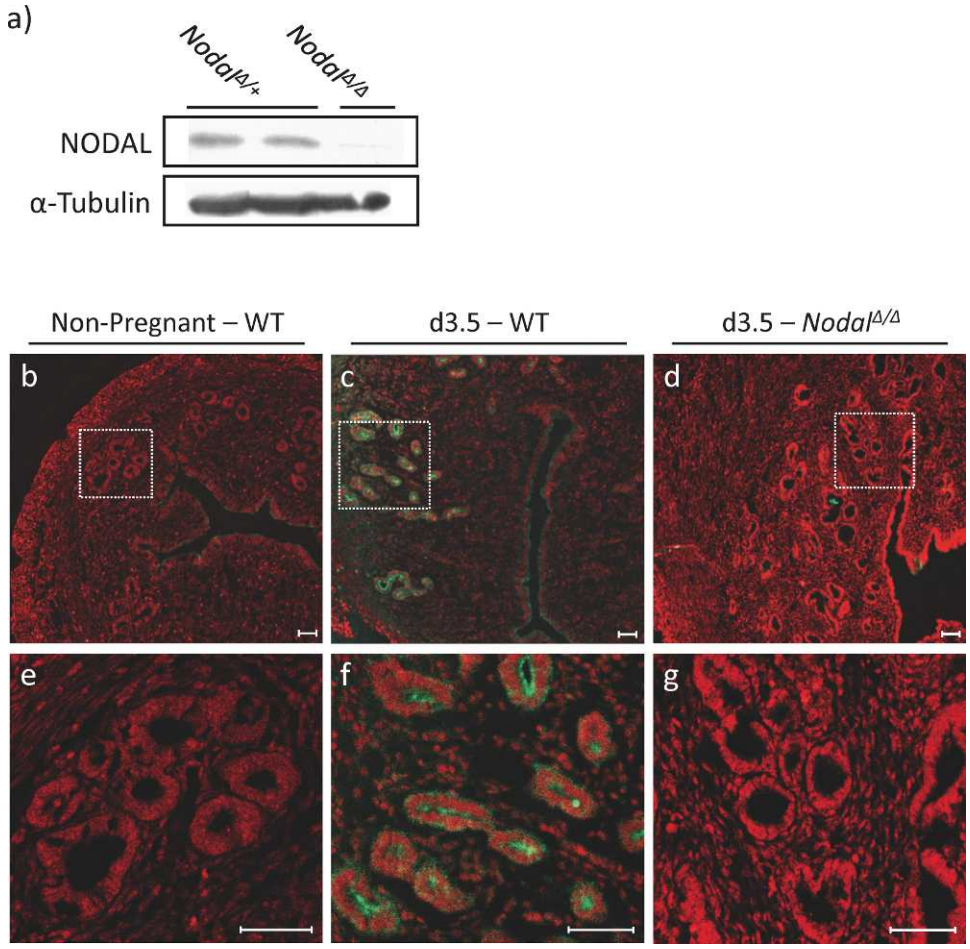

FIG. 1. *Nodal* is effectively deleted in *Nodal*$^{\Delta/\Delta}$ uteri. **a**) Western blotting of total protein isolated from *Nodal*$^{\Delta/\Delta}$ uteri on Day 3.5 postcoitum produced an extremely faint band when probed for NODAL. Conversely, robust NODAL protein was detected in Day 3.5 *Nodal*$^{\Delta/+}$ control uteri. α-Tubulin served as a loading control. As previously published, NODAL protein (green) was undetectable by immunofluorescence in the glandular epithelium of nonpregnant wildtype females (**b** and **e**), whereas a strong signal was observed when uteri were isolated during the peri-implantation period (Day 3.5; **c** and **f**). **d** and **g**) Uterine sections obtained from *Nodal*$^{\Delta/\Delta}$ females on Day 3.5 of pregnancy displayed minimal target staining, indicating efficient knockout of NODAL protein. Sections are counterstained with propidium iodide (red). Bars = 50 μm.

(Fig. 3a). No significant difference was detected in the number of implantation sites recorded on Day 8.5, and the average conceptus site weight was nearly identical (*Nodal*$^{\Delta/+}$, 280.4 mg; *Nodal*$^{\Delta/\Delta}$, 280.7 mg; Fig. 3, b and c, and Supplemental Table S2). Therefore, at the whole-mount level, it appears decidualization and conceptus site growth are unaffected if plugged *Nodal*$^{\Delta/\Delta}$ females overcome the early reproductive phenotype and successfully establish pregnancy.

Fetuses Developing in Pregnant Nodal$^{\Delta/\Delta}$ *Females Experience IUGR During Late Pregnancy*

Fetuses were isolated from *Nodal*$^{\Delta/\Delta}$ knockout and *Nodal*$^{\Delta/+}$ control females and weighed at several time points throughout pregnancy prior to the onset of premature birth (Days 10.5–16.5). Fetuses isolated from *Nodal*$^{\Delta/\Delta}$ females were of comparable size when measured during midpregnancy, with no significant difference observed on Day 10.5 and *Nodal*$^{\Delta/\Delta}$-derived fetuses slightly larger on Day 12.5 (Fig. 4a). However, fetuses obtained from the pregnant *Nodal*$^{\Delta/\Delta}$ females exhibited significant IUGR during the later stages of pregnancy when observed on Days 15.5 and 16.5 ($P < 0.0001$ on Day 15.5/16.5). By Day 16.5, uterine *Nodal* deleted mice contained fetuses that were on average 32.0% smaller than those from the heterozygous control females (*Nodal*$^{\Delta/+}$, 0.609 g; *Nodal*$^{\Delta/\Delta}$, 0.414 g; Fig. 4b and Supplemental Table S3). Examination of the fetuses suggested this restriction is due to inadequate intrauterine growth rather than a developmental defect or delay, because numerous Day 16.5 markers were observed in the *Nodal*$^{\Delta/\Delta}$-derived litters (i.e., asperous skin texture, defined upper lip, paralleled digits). As a result, *Nodal*$^{\Delta/\Delta}$ mothers are unable to support adequate fetal growth during mid to late gestation before the onset of preterm birth.

Placentation in Nodal$^{\Delta/\Delta}$ *Females Is Disrupted*

The timing and severity of IUGR suggest inadequate placenta development might underlie the observed phenotype. Therefore, an extensive histological examination of the extraembryonic tissues during midpregnancy was conducted. Following implantation, no observable differences were discovered in uteri isolated from Day 6.5 *Nodal*$^{\Delta/\Delta}$ and *Nodal*$^{\Delta/+}$ females (Fig. 5, a and b). Embryos appeared morphologically normal, and the area of decidualization (dotted line) was equivalent. On Day 8.5, *Nodal*$^{\Delta/\Delta}$ uterine sections exhibited a slightly larger area of decidualization, with differentiated stromal cells extending further into the lateral and mesometrial endometrium (Fig. 5, c and d).

Interestingly, Day 10.5 uterine sections displayed abnormal trophoblast giant cell layer morphology around the invasive

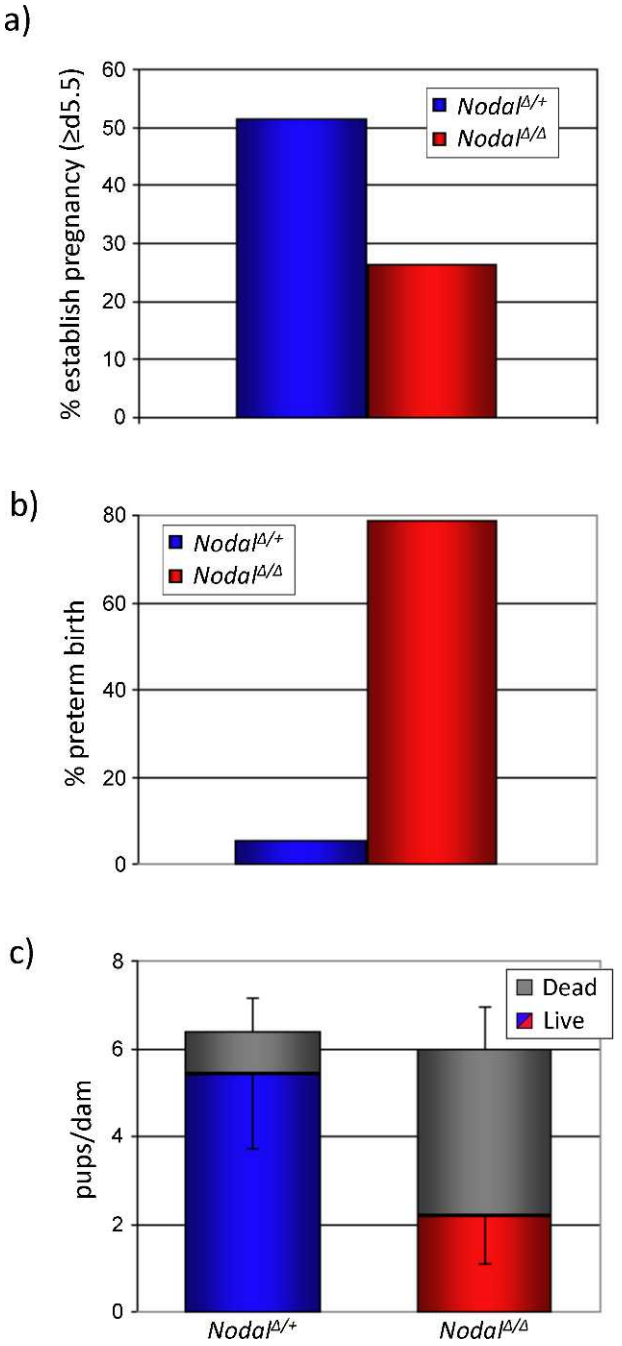

FIG. 2. *Nodal*$^{\Delta/\Delta}$ mice exhibit reduced fertility in addition to preterm birth and fetal loss. Graphical illustration of the results presented in Table 1 and Supplemental Table S1. *Nodal*$^{\Delta/\Delta}$ mice mated with wildtype males displayed a low rate of establishing pregnancy (**a**) due to an early reproductive phenotype (26.3%; n = 19) and experience an increased rate of preterm birth (78.6%; n = 14; **b**) when compared with double-heterozygous *Nodal*$^{\Delta/+}$ control mice. **c**) *Nodal*$^{\Delta/\Delta}$ litters also exhibited increased fetal wastage occurring at or shortly after parturition. Box columns display live pups per dam (bottom, colored) and dead pups per dam (top, gray) for both *Nodal*$^{\Delta/+}$ and *Nodal*$^{\Delta/\Delta}$ litters. Values are mean ± SEM. SEM of dead pups per dam is positioned above the column, and SEM of live pups per dam is positioned within the column.

front of the fetal-derived tissues. Significantly large clusters of giant cells were observed in several *Nodal*$^{\Delta/\Delta}$ uteri along the lateral and antimesometrial surface of the conceptus, expanding at the expense of the stromal compartment, and in a few instances protruding into the embryonic cavity (Fig. 5, e and f). Furthermore, the mesometrial surface of the expanding extra-embryonic tissue appeared to extend deeper into the maternal endometrium, although this phenotype was variable in several samples (Fig. 5, g and h). By Day 12.5, *Nodal*$^{\Delta/\Delta}$ placental sections displayed a striking and significant loss of maternal tissue, primarily the maternal decidua basalis (Fig. 5, i–l). The fetal-derived layers (spongiotrophoblast, labyrinth) comprised most of the uterine *Nodal* deleted placentae, and many samples contained hemorrhaging around the trophoblast giant cell layer that closely apposed the maternal edge of the placenta. Furthermore, *Nodal*$^{\Delta/\Delta}$ placentas became easily detached from the uterus during dissection because of what appears to be a poor integration with the uterine wall. The considerable loss of decidua basalis tissue observed in *Nodal*$^{\Delta/\Delta}$-derived placentae appears to be, to our knowledge, the most severe morphological phenotype to affect the maternal compartment of the mature murine placenta.

The Fetal Layers of the Nodal$^{\Delta/\Delta}$ *Placenta Remain Distinguishable with Moderate Abnormalities*

In order to thoroughly characterize the observed phenotype, Day 12.5 *Nodal*$^{\Delta/\Delta}$ and *Nodal*$^{\Delta/+}$ control placentae were probed by in situ hybridization with numerous fetal layer markers. Prolactin family 3, subfamily d, member 1 (*Prl3d1*); prolactin family 3, subfamily b, member 1 (*Prl3b1*); and prolactin family 2, subfamily c (*Prl2c*) were used to collectively identify parietal (P-), canal (C-), sinusoidal (S-), and spiral artery (SpA-) trophoblast giant cells (TGCs). Using *Prl3d1*, P-TGCs appear, as expected, in a defined layer along the mesometrial aspect of the fetal compartment (Fig. 6, a and b). *Prl3b1*, which in addition to P-TGCs also marks C-TGCs, S-TGCs, and spongiotrophoblasts, displayed moderate disorganization in *Nodal*$^{\Delta/\Delta}$ placenta, because staining appeared to be more robust on the mesometrial surface and extended deeper into the fetal labyrinth (Fig. 6, c and d). However, expression of *Prl2c*, which marks P-TGCs, C-TGCs, SpA-TGCs, and spongiotrophoblasts, remained relatively unaltered, although expression of the *Prl2c* marker is known to diminish considerably by Day 12.5 (Fig. 6, e and f).

Using prolactin family 8, subfamily a, member 8 (*Prl8a8*) and trophoblast-specific protein alpha (*Tpbpa*), two independent probes were used to mark the fetal spongiotrophoblast layer. Interestingly, *Prl8a8* provided minimal staining of the spongiotrophoblast, with no observable differences between the *Nodal*$^{\Delta/+}$ and *Nodal*$^{\Delta/\Delta}$ sections; however, *Tpbpa* displayed a pattern of expression similar to that of the *Prl3b1*, with areas of marked cells observed protruding into the labyrinth (Fig. 6, g–j). By Day 12.5, *Hand1* encompassed all three major fetal layers of the placenta, marking the outer TGCs, spongiotrophoblasts, and labyrinth in both the control and experimental groups (Fig. 6, k and l).

Finally, glial cells missing 1 (*Gcm1*) and cathepsin Q (*Ctsq*) were used to identify various cell types within the labyrinth layer. *Gcm1* is specifically expressed in the chorionic trophoblast cell derivatives in the labyrinth, including mononuclear and syncytial cells that line the maternal blood spaces. As predicted by the spongiotrophoblast layer morphology observed in *Nodal*$^{\Delta/\Delta}$ placentas, *Gcm1* in situ hybridization produced disbanded staining of the complementary tissue in the labyrinth, whereas *Gcm1* remained uniformly distributed in the *Nodal*$^{\Delta/+}$ controls (Fig. 6, m and n). *Gcm1* expression also appears to be more encompassing in the *Nodal* knockout placentae, with an increased number of positively marked cells throughout the labyrinth. Intriguingly, *Ctsq*, marking S-TGCs at the site of nutrient/waste exchange, appears much more

TABLE 1. *Nodal*$^{\Delta/\Delta}$ females experience preterm birth and fetal loss.

Genotype	No. of pregnant females	Time of labor (day)[a,b]				Live pups/dam (mean ± SEM)	Dead pups/dam (mean ± SEM)[c]
		17.5	18.5	19.5	20.5		
Nodal$^{\Delta/+}$	18	0	1	17	0	5.4 ± 1.7	1.0 ± 0.8
Nodal$^{\Delta/\Delta}$	14	9	2	2	1	2.2 ± 1.0	3.8 ± 1.0

[a] Time of labor was defined as the day when the first pup was observed.
[b] Number of females delivering on each day. Frequency of preterm birth (≤Day 18.5 postcoitum) is illustrated in Figure 2b.
[c] Dead pups were defined as stillborn or death within 24 h of delivery. Fetal loss is illustrated in Figure 2c.

robust and appears to encompass a larger portion of the fetal placenta in the uterine *Nodal* knockout samples (Fig. 6, o and p). Taken together, these experiments suggest *Nodal*$^{\Delta/\Delta}$ placenta contain all of the fetal layers within the maturing placenta, but with moderate alterations in layer organization and increased *Gcm1*/*Ctsq*-expressing cells in the labyrinthine compartment.

Maternal Decidua Basalis in the Developing Nodal$^{\Delta/\Delta}$ *Placenta Exhibits Reduced Proliferation and Increased Apoptosis*

As described above, the maternal decidua basalis in *Nodal*$^{\Delta/\Delta}$ placentae becomes severely compromised by Day 12.5. In order to delineate the underlying cause(s) of the altered morphology and to provide insight into potential roles for uterine-derived NODAL, we examined several processes that can alter placental architecture. Using the PCNA marker, immunohistochemistry was performed on Day 10.5 *Nodal*$^{\Delta/\Delta}$ and *Nodal*$^{\Delta/+}$ placental sections. Maternal decidual tissue obtained from *Nodal*$^{\Delta/\Delta}$ females displayed a significantly reduced level of PCNA nuclear staining in comparison with the robust signal observed in *Nodal*$^{\Delta/+}$ controls (Fig. 7, a–c). Interestingly, uterine tissue immediately adjacent to the muscular myometrium appears relatively unaffected, whereas only a limited number of proliferating cells were observed in the central (Fig. 7, d–f) and antimesometrial (Fig. 7, g–i) decidua basalis of *Nodal*$^{\Delta/\Delta}$-derived placenta. In contrast, no difference in marker staining was detected in the fetal trophoblast giant cell, spongiotrophoblast, or labyrinth layers. Immunohistochemistry was also

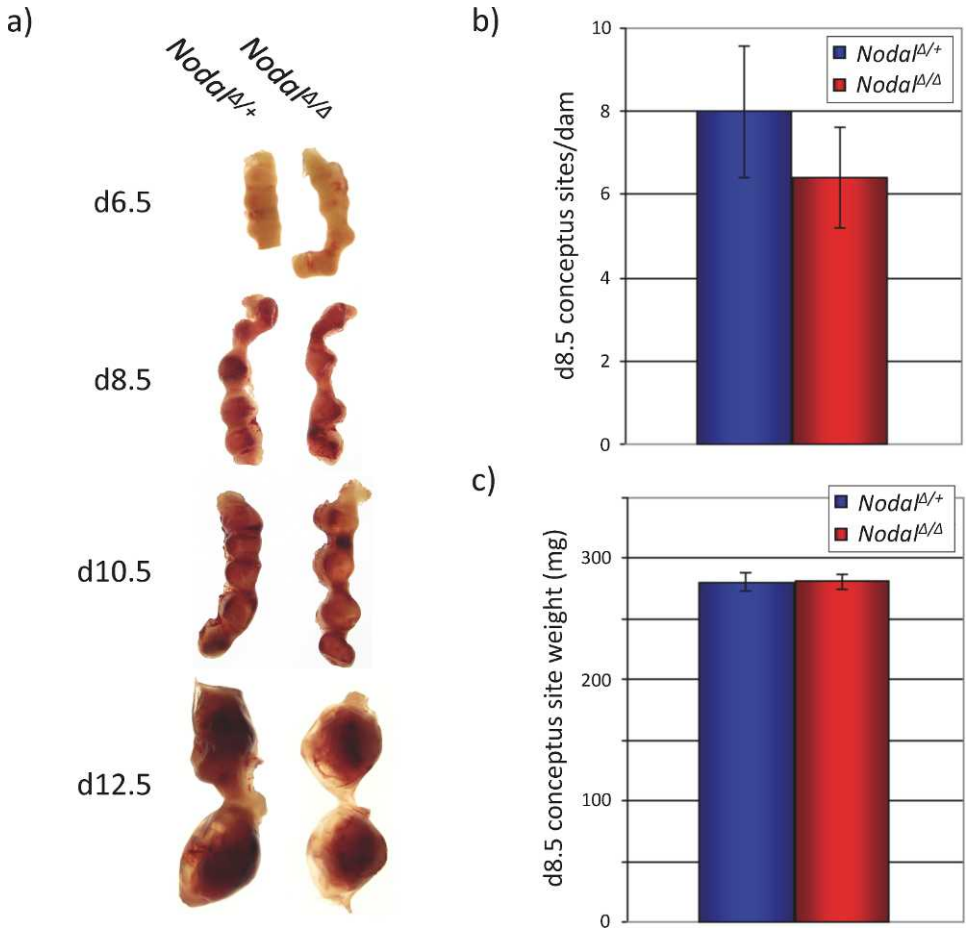

FIG. 3. Uterine deletion of *Nodal* does not affect postimplantation decidualization ability. **a**) Whole-mount uteri isolated from pregnant *Nodal*$^{\Delta/+}$ and *Nodal*$^{\Delta/\Delta}$ females on Days 6.5–12.5 postcoitum depicting relative size and quality of conceptus sites. Photographs of compared uteri were taken in the same photographic frame. If pregnancy is obtained, the number (**b**) and weight (**c**) of the conceptus site are unaffected in *Nodal*$^{\Delta/\Delta}$ females when quantified on Day 8.5. Complete data are presented in Supplemental Table S2. Values are mean ± SEM.

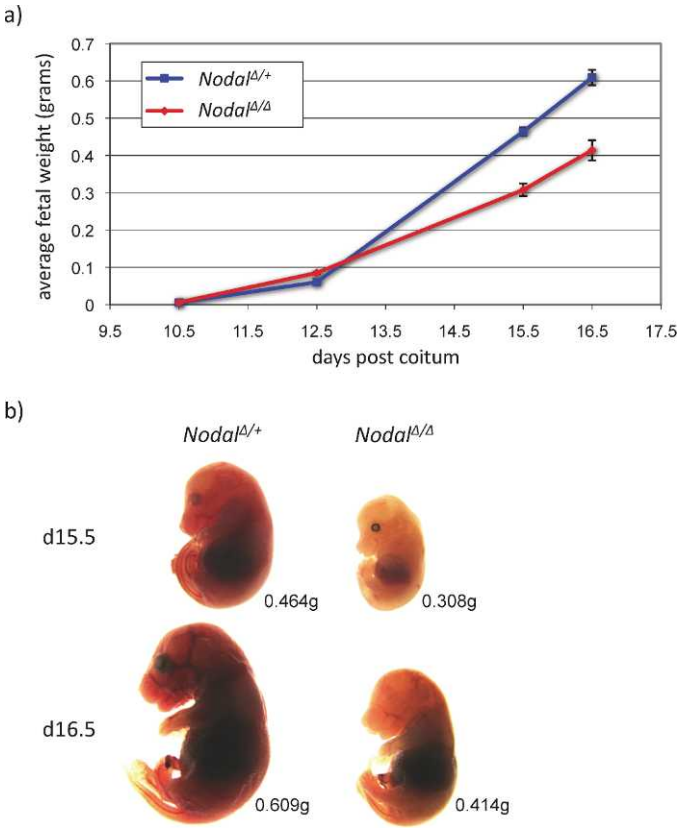

FIG. 4. Fetuses developing in uterine *Nodal* deleted females exhibit IUGR prior to parturition. **a**) Growth curve illustrating the fetal weight of offspring derived from *Nodal*$^{\Delta/+}$ and *Nodal*$^{\Delta/\Delta}$ females during mid and late pregnancy. Experimental *Nodal*$^{\Delta/\Delta}$ mothers contain fetuses of similar weight on Day 10.5, but growth is compromised by Day 15.5 postcoitum. Complete data are presented in Supplemental Table S3. Values are mean ± SEM. **b**) Photographic representation of average fetus size on Days 15.5 and 16.5 from *Nodal*$^{\Delta/+}$ and *Nodal*$^{\Delta/\Delta}$ females. Specimens were photographed in the same frame, thereby depicting relative size.

performed with an alternate proliferation marker, MKI67, generating a similar pattern of expression with a marked reduction in decidua basalis expression (Supplemental Fig. S1).

In addition to proliferation, the effects of uterine *Nodal* deletion on apoptosis were investigated by in situ TUNEL assay on Day 10.5 placental sections. Strikingly, few apoptotic cells were detected in placentas isolated from *Nodal*$^{\Delta/+}$ controls; however, abundant positively marked cells were observed throughout the maternal decidua basalis in *Nodal*$^{\Delta/\Delta}$ placentae (Fig. 8). Interestingly, a high concentration of apoptotic cells was positioned adjacent to the mesometrial aspect of the trophoblast giant cell layer. For example, several sections displayed numerous positive cells situated between the giant cell layer and uterine lumen (Fig. 8h). Taken together, the reduced maternal decidua basalis appears to be the product of reduced proliferation combined with increased cell death prior to Day 12.5 postcoitum.

The Parturition Cascade in Pregnant Nodal$^{\Delta/\Delta}$ *Females Is Disrupted prior to the Onset of Labor*

In mice, parturition is known to be regulated at the maternal-fetal interface by the production of prostaglandins derived from the cyclooxygenase (COX or PTGS)/PGFS/PGF_{2a} signaling axis [22]. Briefly, the COX enzymes convert arachidonic acid to PGH_2, which is then converted to PGF_{2a}, PGE_2, and PGI_2 by their respective PG synthases (PGFS, mPGES1, and PGIS). Ultimately, the production of PGF_{2a} results in luteolysis of the ovarian corpora lutea, and subsequently a drop in maternal blood serum progesterone levels. This progesterone withdrawal is absolutely essential in mice for the cervical ripening and uterine contractions that precede birth [23]. Although several components of the parturition cascade have been identified, the precise molecular events that initiate natural parturition remain poorly understood. As a result, our ability to determine the underlying causes and contributing factors of spontaneous and idiopathic preterm birth is limited. As *Nodal*$^{\Delta/\Delta}$ females experience aberrant placentation leading to a disrupted maternal-fetal interface prior to the onset of preterm birth, it is possible the parturition cascade has been affected or prematurely initiated because of *Nodal* deletion. Therefore, assessing the known components of the parturition cascade is a critical primary step toward using the *Nodal*$^{\Delta/\Delta}$ strain to elucidate the underlying mechanics of preterm birth.

In order to determine whether the documented components of the parturition cascade are disrupted prior to preterm birth in *Nodal*$^{\Delta/\Delta}$ females, we first quantified the level of PTGS2 enzyme at the maternal-fetal interface. Interestingly, we observed a significant 2-fold increase of PTGS2 protein within the maternal tissues of *Nodal*$^{\Delta/\Delta}$ females when quantified by Western blot analysis on Day 16.5 ($P < 0.02$; Fig. 9a). As a result, histological sections of the ovarian tissue were analyzed and the progesterone concentration in maternal blood serum was quantified by radioimmunoassay. Although we were unable to directly observe luteolysis by histological sectioning (Fig. 9b) or in situ TUNEL assay (data not shown), a significant decline in progesterone concentration was observed prior to preterm birth in the *Nodal*$^{\Delta/\Delta}$ group (*Nodal*$^{\Delta/+}$, 46.87 ± 8.27 ng/ml; *Nodal*$^{\Delta/\Delta}$, 28.58 ± 3.96 ng/ml; Fig. 9c). Furthermore, four of five blood samples collected from *Nodal*$^{\Delta/\Delta}$ females on Day 16.5 had a considerably lower progesterone concentration (<28.0 ng/ml; 0.59-fold) than the mean concentration observed in the control group. As a result, premature progesterone withdrawal occurs in a proportion of the pregnant *Nodal*$^{\Delta/\Delta}$ population that correlates with the observed rate of preterm birth (11 of 14 preterm; Fig. 2b). These observations indicate that deleting *Nodal* from the uterus ultimately contributes to a disrupted parturition cascade, leading to an early decline in maternal progesterone and, as a result, preterm birth. Interestingly, the precise point of deviation from the natural cascade occurs upstream of PTGS2 production, extending beyond the well-documented events that are known to mediate parturition.

DISCUSSION

In this study, we describe the generation of a novel transgenic mouse strain with a maternal-specific deletion of *Nodal* that displays aberrant placentation, ultimately leading to significant IUGR, preterm birth, and fetal loss. The role of NODAL in facilitating placental development has remained a well-studied topic in trophoblast research; however, most of these studies focus on the role of NODAL derived from an embryonic origin. Indeed, complete ablation of the *Nodal* gene, in addition to disrupting primitive streak and mesoderm formation, also results in impaired extraembryonic tissues with an increased giant cell number and a loss of spongiotrophoblast and labyrinth [7, 24]. Furthermore, NODAL hypomorphic mice that prolong embryo development beyond chorioallantoic fusion before the onset of lethality also display an expanded giant cell and reduced labyrinth, but unexpectedly contain a larger spongiotrophoblast compartment [25]. The authors of these studies hypothesize that embryonic NODAL may be

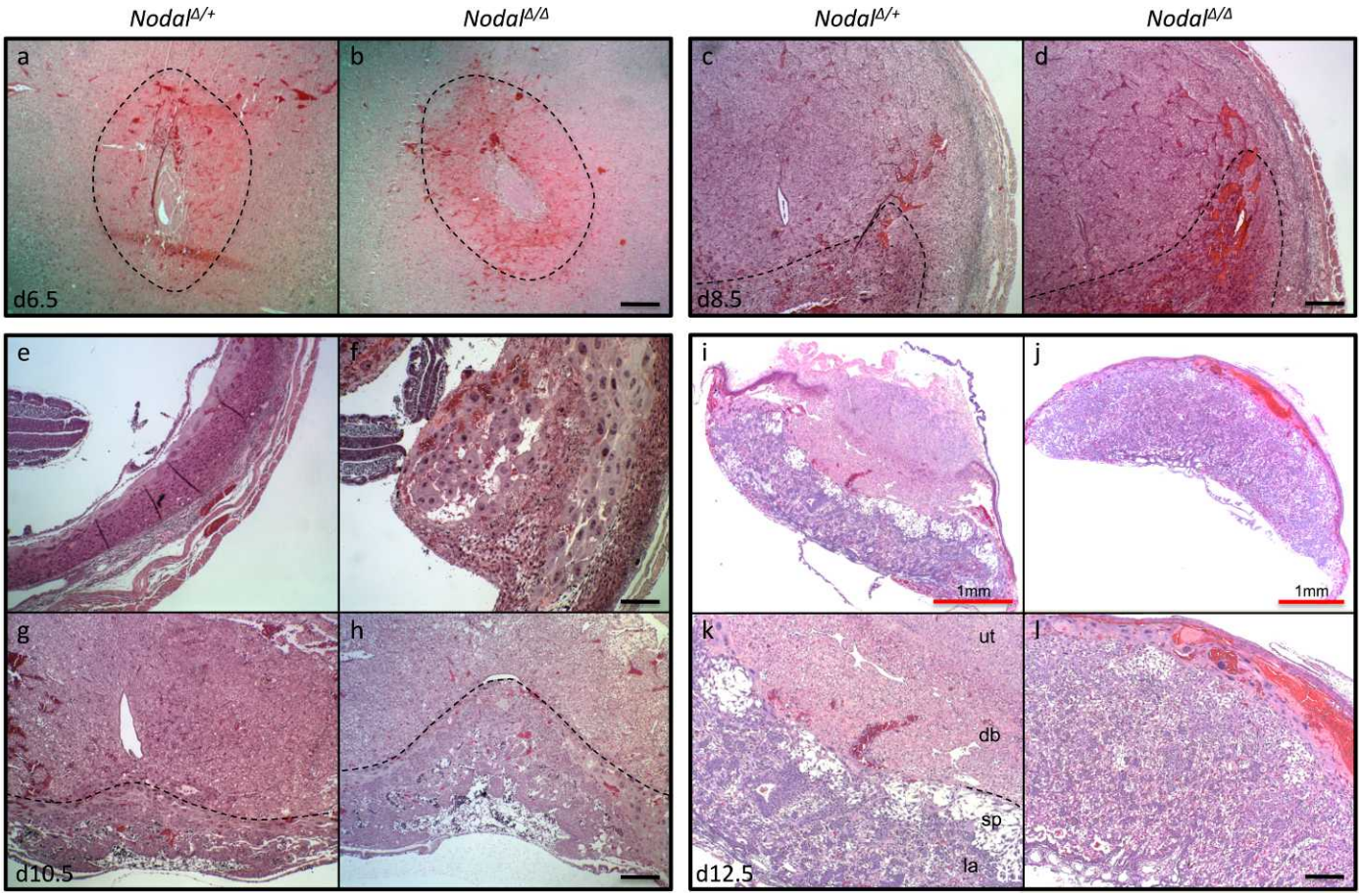

FIG. 5. Histological examination of pregnant *Nodal*$^{\Delta/\Delta}$ uteri reveals aberrant placentation. Transverse sections through the conceptus site of *Nodal*$^{\Delta/\Delta}$ and *Nodal*$^{\Delta/+}$ uteri displayed no difference in the area of decidualization (dotted line) on Day 6.5 (**a** and **b**) and a slightly larger decidual zone in *Nodal*$^{\Delta/\Delta}$ uteri isolated on Day 8.5 (**c** and **d**). **e** and **f**) On Day 10.5, samples isolated from *Nodal*$^{\Delta/\Delta}$ uteri exhibited abnormal trophoblast giant cell expansion along the mesometrial and lateral surfaces of the conceptus site. **g** and **h**) In several *Nodal*$^{\Delta/\Delta}$ samples, the invasive front of the fetal layer (dotted line) extended deeper into the maternal compartment in comparison with *Nodal*$^{\Delta/\Delta}$ control sections. Low (**i** and **j**) and high (**k** and **l**) magnifications of Day 12.5 transverse sections through the center of *Nodal*$^{\Delta/+}$ and *Nodal*$^{\Delta/\Delta}$ placentae display a significant loss of the maternal decidua basalis, hemorrhaging along the mesometrial surface, and a poor integration with the uterine endometrium. All sections are stained with hematoxylin and eosin. In **k**: ut, uterus; db, decidua basalis; sp, spongiotrophoblast; la, labyrinth; dotted line, parietal trophoblast giant cell layer. Bars = 200 μm unless otherwise indicated.

involved in redirecting trophoblast fate toward an expansion of the labyrinth while maintaining a thin layer of trophoblast giant cells at the maternal-fetal boundary [26]. More recently, NODAL has been shown to be essential for the in vivo maintenance of the trophoblast stem cell microenvironment by preventing precocious differentiation; however, this role is likely mediated indirectly through FGF4 produced in the embryonic ectoderm [27, 28].

The results presented in this study add a new and important dimension to the role of NODAL signaling during placenta development, because eliminating the uterine contribution of NODAL to the maternal-fetal interface has severe consequences on placentation and reproductive outcome. Strikingly, the placenta of *Nodal*$^{\Delta/\Delta}$ mice have a significantly diminished maternal decidua basalis, and in a few cases displayed irregular extraembryonic characteristics, such as an expanded trophoblast giant cell layer or moderate spongiotrophoblast/labyrinthine disorganization. Further investigation of the underlying mechanics revealed that increased apoptosis and reduced proliferation within the maternal compartment contributed to the decidua basalis deletion by midgestation (Day 12.5 postcoitum). Several reports have previously implicated the NODAL signaling pathway in mediating apoptosis and proliferation, although the effect of NODAL appears to vary with cell type. For example, Munir et al. [29] demonstrated that *Nodal* overexpression, acting through activin receptor-like kinase 7 (ALK7) and SMAD2/3, induces apoptosis and inhibits proliferation in human trophoblast cells in vitro (HTR8/SVNeo). Similar proapoptotic effects of *Nodal* overexpression were also observed in human epithelial ovarian cancer cells [30] and rat ovarian granulosa cells during follicular atresia [31]. However, the opposite effect was observed in orthotopic human breast cancer cells (MDA-MB-231) and melanoma tumors (C8161), because inhibition of NODAL decreased proliferation (as marked by MKI67) and increased apoptosis (TUNEL) [32]. Apoptosis is also extensive in embryonic *Nodal* mutants on Day 7.5 that fail to undergo mesoderm differentiation, leading the authors to suggest the loss of NODAL signal leads directly to programmed cell death of precursor ectodermal cells [33]. As presented here, the loss of maternal NODAL from the uterus during pregnancy appears to have the latter effect in vivo, because increased apoptosis and decreased proliferation lead to a significant reduction of decidua basalis tissue during placentation.

It is well documented that maternal-fetal interactions are critical for the establishment of pregnancy and generation of a healthy placenta [34, 35]. As placentation proceeds, NODAL is observable in both the developing fetal and maternal compart-

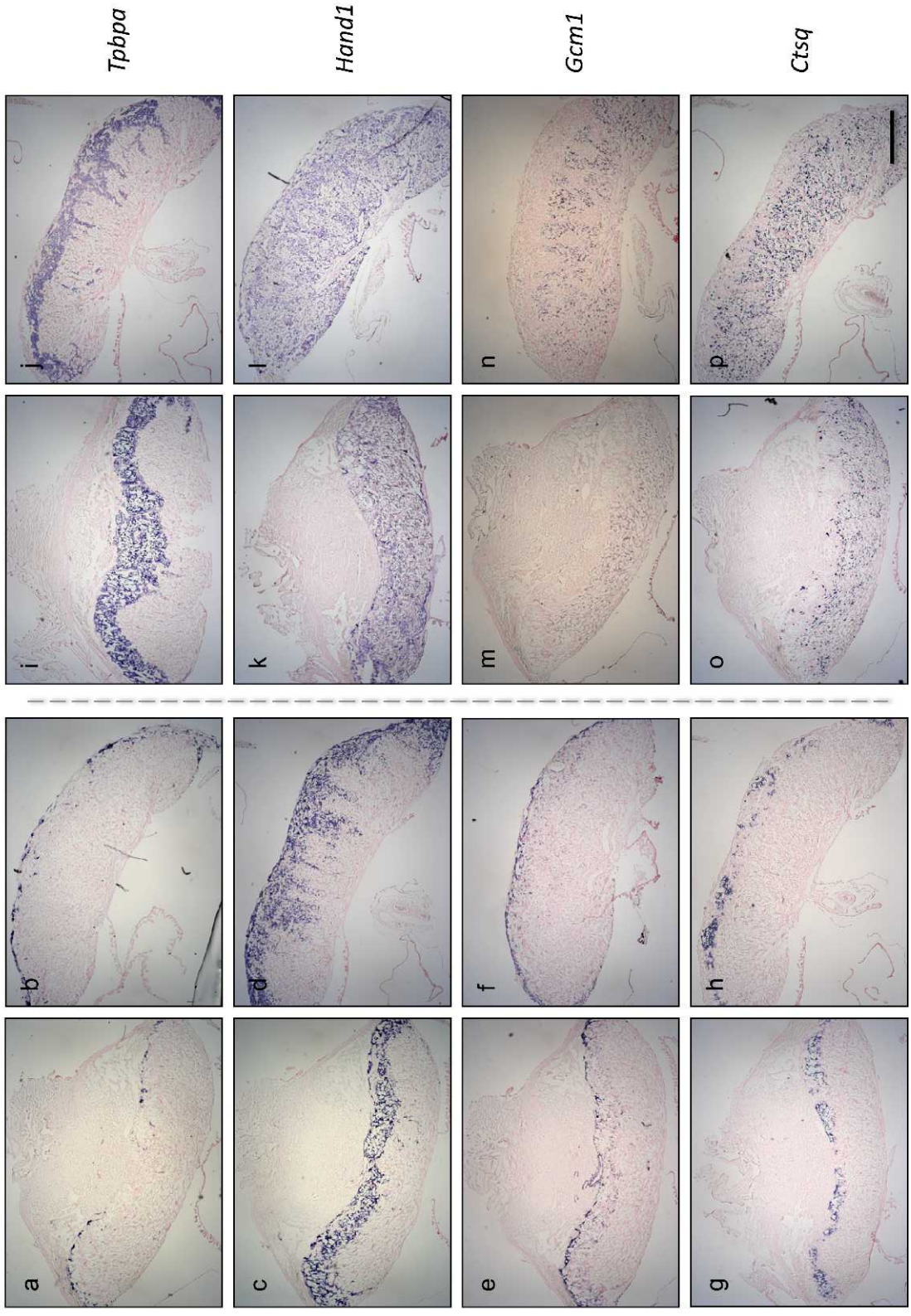

FIG. 6. In situ hybridization marker analysis of the fetal layers in mature Day 12.5 $Nodal^{\Delta/+}$ and $Nodal^{\Delta/\Delta}$ placental sections. **a** and **b**) *Prl3d1* marking P-TGCs. **c** and **d**) *Prl3b1* depicting P-TGCs, C-TGCs, and S-TGCs. **e** and **f**) *Prl2c* marking P-TGCs, SpA-TGCs, and spongiotrophoblasts. Although *Prl3d1* and *Prl2c* expression appears unaltered, moderate abnormalities are highlighted with *Prl3b1* staining, suggesting increased C-TGCs and/or S-TGCs contained in the fetal compartment of $Nodal^{\Delta/\Delta}$ samples. *Prl8a8* (**g** and **h**) and *Tpbpa* (**i** and **j**) expression used to mark the spongiotrophoblast layer. Although *Prl8a8* produced limited staining that was similar in both $Nodal^{\Delta/+}$ and $Nodal^{\Delta/\Delta}$ placentas, *Tpbpa* expression displayed spongiotrophoblast cells protruding into the labyrinth layer. **k** and **l**) *Hand1* expression, used to mark outer TGCs, spongiotrophoblasts, and labyrinth, was unaltered in the $Nodal^{\Delta/\Delta}$ fetal compartment; however, the staining pattern highlights the lack of integration with the maternal uterine endometrium. *Gcm1* (**m** and **n**) and *Ctsq* (**o** and **p**) expression, marking various cells within the labyrinth, displayed more encompassing and robust signals in $Nodal^{\Delta/\Delta}$ knockout placenta in comparison with the $Nodal^{\Delta/+}$ control sections with moderate staining. All sections are counterstained with Nuclear Fast Red. Bars = 1 mm.

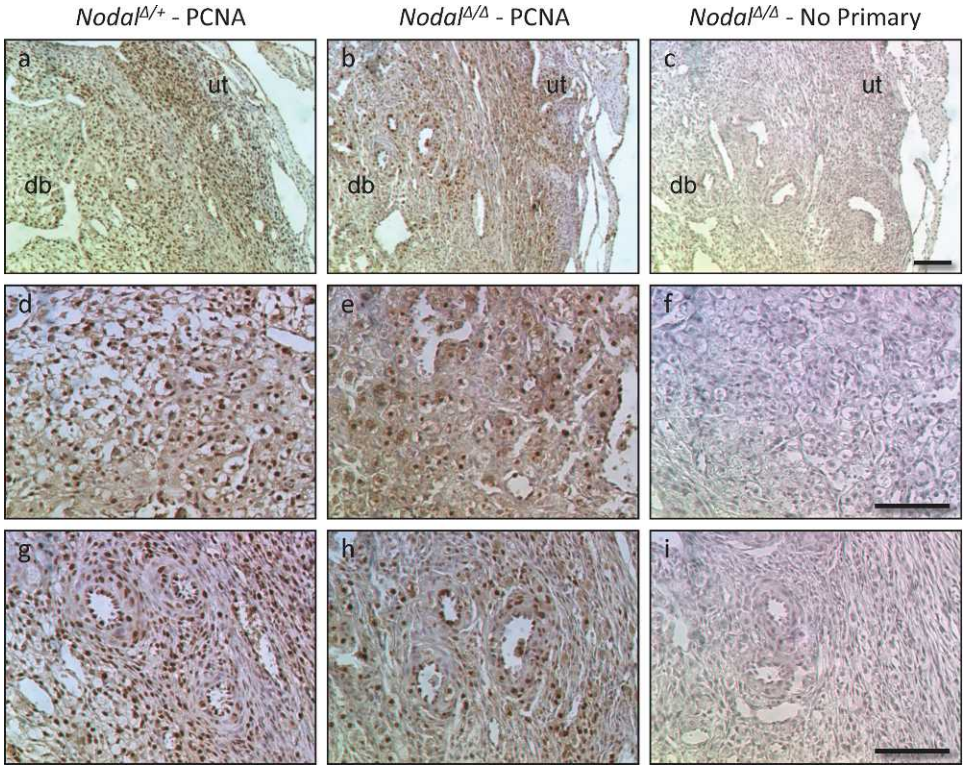

FIG. 7. Proliferation is reduced in the maternal decidua basalis of uterine *Nodal*$^{\Delta/\Delta}$ knockout placenta. **a** and **b**) Immunohistochemistry for the proliferation maker, PCNA, displayed fewer positively marked cells (brown) in the decidua basalis layer of placenta isolated from *Nodal*$^{\Delta/\Delta}$ females on Day 10.5 post coitum. Higher-magnification view of the central (**d** and **e**) and antimesometrial (**g** and **h**) aspect of the decidua basalis compartment demonstrated robust *Nodal*$^{\Delta/+}$ and limited *Nodal*$^{\Delta/\Delta}$ PCNA localization. **c**, **f**, and **i**) No primary antibody negative control sections. Tissue sections are counterstained with hematoxylin. ut, uterus; db, decidua basalis. Bars = 100 μm.

ments, because expression has been detected in the ectoplacental cone, chorion (Day 8.5), and spongiotrophoblast (≥Day 10.5) in addition to the uterine stroma (Day 8.5) and decidua parietalis (≥Day 10.5) [12, 26, 28]. As such, it is an interesting observation that *Nodal*$^{\Delta/\Delta}$ placentae, much like embryonic *Nodal* mutants, exhibited drastic trophoblast giant cell clustering along the maternal-fetal border on Day 10.5. Although, unexplainably, less apparent on Day 12.5 in *Nodal*$^{\Delta/\Delta}$ placenta and uncharacterized in null *Nodal* placenta because of embryonic lethality, this phenotype supports the initial function of NODAL hypothesized by Ma et al. [26] with regard to maintaining a thin giant cell layer. The morphogenic properties and self-regulating positive/negative feedback loops associated with NODAL signaling make it tempting to hypothesize that a delicate balance of NODAL signal along, or across, the maternal-fetal interface is critical for placenta development [10]. Perhaps, endogenous NODAL protein from both fetal and maternal sources maintains proper placenta histoarchitecture, and disrupting this balance (from either source) severely affects placenta layer formation, as evident from both the *Nodal* null females described above and the uterine *Nodal*$^{\Delta/\Delta}$ mice characterized in this study. Although an interesting possibility, it remains to be seen if deleting embryonic or maternal NODAL alters the expression profile of NODAL in neighboring tissue compartments.

Following the placenta malformation, several phenotypes arise during late pregnancy as an apparent result of this placental insufficiency. First, we observed significant IUGR of fetuses developing within the uterine *Nodal* deleted females. As the source of the nutrients and gas exchange required for fetal development, it is easy to speculate that aberrant placentation led to insufficient nourishment and stunted growth. However, the precise underlying cause(s) remains to be determined. Interestingly, more expansive *Ctsq* expression, a marker of syncytiotrophoblast cells (SynT-Is), and *Gcm1* were observed in the labyrinth of *Nodal*$^{\Delta/\Delta}$ placentae. Considering functionality, it is not inconceivable that *Nodal*$^{\Delta/\Delta}$ placenta may have adapted an expanded labyrinth and/or increased the surface of maternal-fetal exchange to compensate for a reduced supply of maternal blood. As one would expect, fetal growth restriction has been associated with a diminished labyrinth phenotype [36]; however, IUGR has also been observed alongside a significantly larger labyrinth layer in the stroptozocin-induced diabetic rat [37]. However, in the diabetic rat strain a thickening of the trophoblastic layers within the labyrinth was also observed and the IUGR was attributed to poor placental transfer.

During proper placental development, the most significant process to occur within the maternal uterine/decidual tissue is the remodeling of the spiral arteries by invading trophoblast cells [38, 39]. During midgestation in mice, a subpopulation of interstitial and endovascular trophoblasts invade the maternal compartment and replace the smooth muscle cells that line the uterine arteries, thereby increasing blood flow for nourishment and rendering the arteries unresponsive to maternal vasoconstriction [40]. Although it has yet to be investigated, it is possible this process is compromised in *Nodal*$^{\Delta/\Delta}$-derived conceptus, because placentae display a diminished decidua basalis. By removing this decidua layer, invading trophoblasts would undoubtedly experience a different physical route to the uterine arteries in addition to a potentially alternate milieu of cytokines, growth factors, hormones, or other influencing factors (μNK cells) present in the decidual layer. Inadequate or

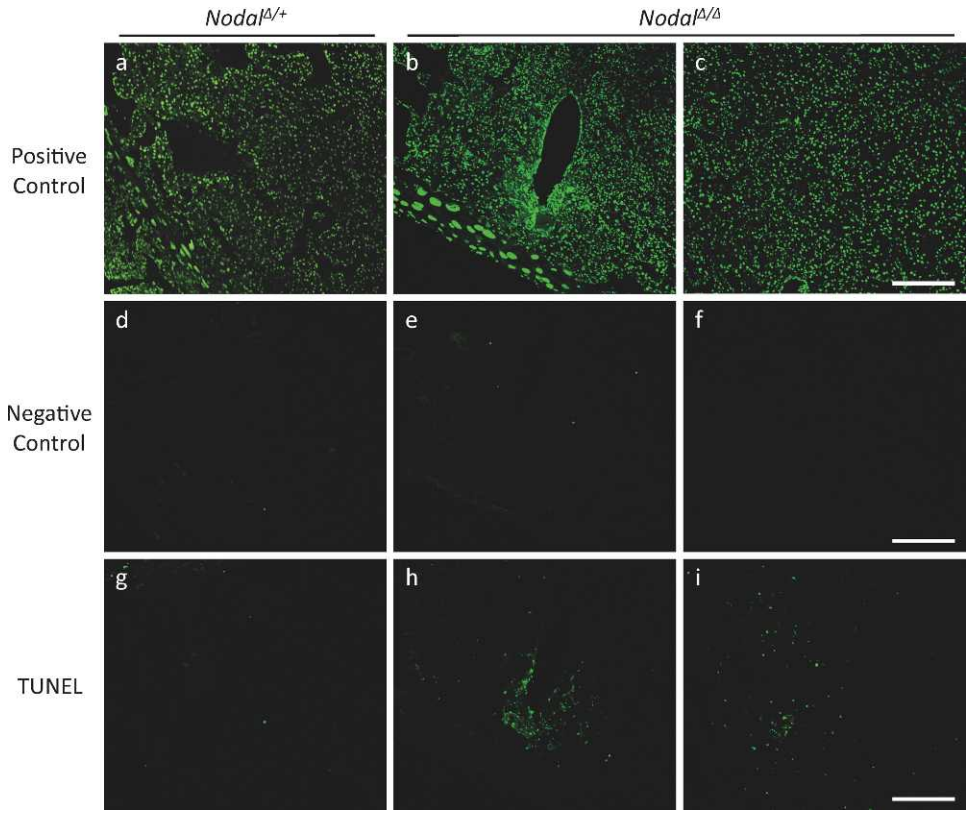

FIG. 8. Apoptosis is increased in the maternal decidua basalis as a result of uterine *Nodal* deletion. Immunofluorescent in situ cell death assay marked all nuclei in DNase I-treated positive control placentas isolated from both *Nodal*$^{\Delta/+}$ (**a**) and *Nodal*$^{\Delta/\Delta}$ (**b** and **c**) females on Day 10.5. **d**–**f**) Minimal to no signal was observed in negative control samples treated without the incorporating enzyme. Experimentally treated sections (TUNEL) displayed minimal staining in *Nodal*$^{\Delta/+}$ control samples (**g**), whereas *Nodal*$^{\Delta/\Delta}$ placenta (**h** and **i**) contained abundant positively marked nuclei in the maternal decidua basalis. Apoptotic cells appeared most concentrated around the antimesometrial (bottom left) aspect of the decidua basalis adjacent to the fetal layers. Bars = 200 μm.

shallow invasion may impede blood delivery, whereas increased trophoblast migration could result in uterine hemorrhaging [41]. Interestingly, NODAL signaling itself has recently been implicated in trophoblast migration and invasion. Using both human trophoblast cell culture and first-trimester placental explants in vitro, it was demonstrated that NODAL signals through ALK7 to inhibit both the migratory ability of trophoblast cells and outgrowth of placenta explants [42]. The opposite effect was observed in siRNA knockdown of either *Nodal* or *Alk7* [42]. Although the precise role of NODAL signaling, whether from embryonic or maternal sources, in mediating trophoblast invasion remains to be determined in mice in vivo, it is an interesting link that *Nodal*$^{\Delta/\Delta}$ females did not support adequate fetal growth during late mid to late pregnancy and also displayed examples of hemorrhaging. As previously discussed, it is possible a complex relationship between the fetal- and maternal-derived NODAL signals plays a critical role in regulating the ability, rate, route, or depth to which trophoblasts invade into the uterine tissue.

The most significant phenotype observed in pregnant *Nodal*$^{\Delta/\Delta}$ females was substantial preterm birth and fetal loss on Day 17.5 of gestation, a phenotype rarely observed in rodents [15]. Strikingly, the only mouse strain to our knowledge that exhibited spontaneous preterm birth also displayed a decreased decidual layer in the mature placenta; however, the reduction appears less pronounced and developed from a different mechanism [43]. By using the same PR-Cre strain and generating a uterine-specific *Trp53* knockout strain, Hirota et al. [43] observed terminal differentiation and cellular senescence of uterine decidua cells, leading to reduced decidua basalis and a compromised maternal-fetal interface. Regression of the decidua basalis occurs naturally in rodents during the second half of pregnancy, and as a result the malformations leading to a reduced decidua tissue coincidentally resemble the histoarchitecture of a late-stage placenta around the time of parturition [44, 45]. Moreover, injection of the bacteria *Fusobacterium nucleatum*, which has been isolated in the amniotic fluid of women delivering prematurely, causes preterm fetal loss in mice [46]. Interestingly, the bacterial infection was first restricted to the lower maternal decidua basalis, where severe inflammation and necrosis were observed before infection spread to neighboring tissues (marginal zone, visceral yolk sac, and amnion) [46]. Taken together, these results suggest prematurely compromising the functional ability of the decidua basalis, whether by deletion or bacterial infection, may lead to preterm delivery and fetal loss in mice. Because the maternal tissue at the placental interface is believed to be the source of the signal(s) that initiate parturition, it is tempting to speculate that abundant, healthy cells within the decidua basalis prevent the production of downstream prostaglandins prior to term, which is then removed naturally during basalis regression.

In the *Nodal*$^{\Delta/\Delta}$ females, much like the uterine *Trp53*-deleted mice, we observed an increase of PTGS2 enzyme at the placental interface; however, this was accompanied by a significant decrease in progesterone concentration in circulating maternal blood that was not observed in Hirota et al. [43]. As a result, uterine deletion of *Trp53* led to dystocia because

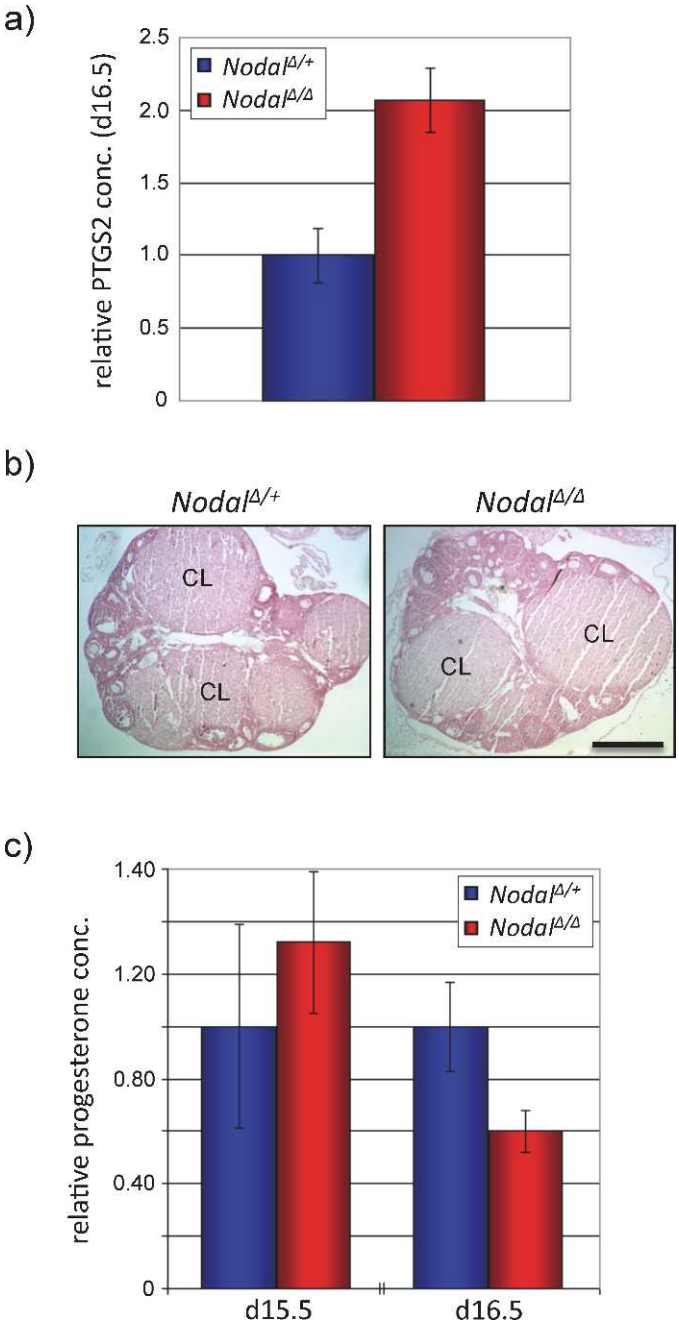

FIG. 9. Uterine *Nodal*$^{\Delta/\Delta}$ deletion results in disrupted components of the parturition cascade prior to the onset of preterm birth. **a**) Quantification of PTGS2 protein isolated from combined maternal and fetal tissue (fetus removed) of Day 16.5 uteri demonstrated a significant 2.07-fold increase in *Nodal*$^{\Delta/\Delta}$ females ($P < 0.02$). **b**) Histological sections of ovarian tissue isolated from *Nodal*$^{\Delta/+}$ and *Nodal*$^{\Delta/\Delta}$ females on Day 16.5 postcoitum displayed ample corpora lutea (CL). Bar = 500 μm. **c**) Relative progesterone quantification during late pregnancy demonstrated a nonsignificant increase on Day 15.5 (1.32-fold) and a significant decrease on Day 16.5 (0.60-fold) postcoitum ($P < 0.05$).

uterine contractions occurred without cervical ripening, whereas *Nodal*$^{\Delta/\Delta}$ mice appeared to deliver without any prolonged distress. This suggests *Nodal*$^{\Delta/\Delta}$ females, although delivering preterm, may have more closely followed the natural parturition cascade once initiated, complete with progesterone withdrawal and a prepared cervix. The precise point at which the preterm induction of parturition deviates from the natural cascade of events remains to be determined; however, it occurs prior to PTGS2 upregulation and appears to be associated with aberrant placental development. Consequently, the newly generated uterine *Nodal*$^{\Delta/\Delta}$ knockout mouse strain provides an attractive alternative for preterm birth research as current models, induced by local bacterial inoculation, fail to address the underlying cause(s) of spontaneous and idiopathic preterm birth. The placenta has long been targeted as a major potential contributor to the pathogenesis of premature delivery and adverse conditions associated with pregnancy [47]. Here, we demonstrate that mice lacking a uterine source of NODAL fail to support adequate placental development though mid-gestation, and ultimately experience a spontaneous premature induction of parturition, leading to fetal loss. Complete characterization of the *Nodal*$^{\Delta/\Delta}$ strain is imperative to the ongoing pursuit of 1) identifying the transduction pathways associated with premature birth and 2) the development of suitable animal models required to advance preterm birth research.

Despite the prevalence, severity, and economic impact of premature birth, very little is understood regarding the causes and mechanisms underlying spontaneous preterm birth. In this study, we describe the generation and analysis of a novel tissue-specific knockout of *Nodal* in the female reproductive tract of mice. Our results demonstrate that NODAL signaling, emanating from a maternal source in the uterus, is critical for proper placental development, adequate intrauterine growth, and term delivery of healthy offspring. These observations shed new light on the in vivo role of maternal NODAL in the developing placenta, present an interesting link between disrupted decidua basalis formation and premature parturition, and introduce a potentially valuable model toward understanding the complex processes that trigger preterm birth.

ACKNOWLEDGMENT

We thank E.J. Robertson for donating the mouse strains required to generate the *Nodal*$^{\Delta/\Delta}$ line; J. C. Cross, D. R. Natale, and M. Gasperowicz for assistance with the in situ hybridization procedure/interpretation; and E. Asselin and S. Parent for assistance with apoptosis experiments and interpretation of the data. We would also like to thank B. D. Murphy and his laboratory for help with the progesterone assays.

REFERENCES

1. Goldenberg RL, Culhane JF, Iams JD, Romero R. Epidemiology and causes of preterm birth. Lancet 2008; 371:75–84.
2. McCormick MC. The contribution of low birth weight to infant mortality and childhood morbidity. N Engl J Med 1985; 312:82–90.
3. Mitchell BF, Taggart MJ. Are animal models relevant to key aspects of human parturition? Am J Physiol Regul Integr Comp Physiol 2009; 297: R525–R545.
4. Als H, Behrman R, Checchia P, Denne S, Dennery P, Hall CB, Martin R, Panitch H, Schmidt B, Stevenson DK, Vila L. Preemie abandonment?: multidisciplinary experts consider how to best meet preemies needs at ''preterm infants: a collaborative approach to specialized care'' roundtable. Mod Healthc 2007; 37:17–24.
5. Moster D, Lie RT, Markestad T. Long-term medical and social consequences of preterm birth. N Engl J Med 2008; 359:262–273.
6. Behrman RE, Butler AS. Preterm Birth: Causes, Consequences, and Prevention. Washington, DC: National Academies Press; 2007.
7. Iannaccone PM, Zhou X, Khokha M, Boucher D, Kuehn MR. Insertional mutation of a gene involved in growth regulation of the early mouse embryo. Dev Dyn 1992; 194:198–208.
8. Brennan J, Norris DP, Robertson EJ. Nodal activity in the node governs left-right asymmetry. Genes Dev 2002; 16:2339–2344.
9. Shen MM. Nodal signaling: developmental roles and regulation. Development 2007; 134:1023–1034.
10. Schier AF. Nodal morphogens. Cold Spring Harb Perspect Biol 2009; 1: a003459.
11. Park CB, Dufort D. Elsevier trophoblast research award lecture: the

multifaceted role of Nodal signaling during mammalian reproduction. Placenta 2011; 32(suppl 2):125–129.
12. Park CB, Dufort D. Nodal expression in the uterus of the mouse is regulated by the embryo and correlates with implantation. Biol Reprod 2011; 84:1103–1110.
13. Papageorgiou I, Nicholls PK, Wang F, Lackmann M, Makanji Y, Salamonsen LA, Robertson DM, Harrison CA. Expression of nodal signalling components in cycling human endometrium and in endometrial cancer. Reprod Biol Endocrinol 2009; 7:122.
14. Ilekis JV, Reddy UM, Roberts JM. Preeclampsia–a pressing problem: an executive summary of a National Institute of Child Health and Human Development workshop. Reprod Sci 2007; 14:508–523.
15. Elovitz MA, Mrinalini C. Animal models of preterm birth. Trends Endocrinol Metab 2004; 15:479–487.
16. Lu CC, Robertson EJ. Multiple roles for Nodal in the epiblast of the mouse embryo in the establishment of anterior-posterior patterning. Dev Biol 2004; 273:149–159.
17. Soyal SM, Mukherjee A, Lee KY, Li J, Li H, DeMayo FJ, Lydon JP. Cre-mediated recombination in cell lineages that express the progesterone receptor. Genesis 2005; 41:58–66.
18. Mukherjee A, Amato P, Allred DC, DeMayo FJ, Lydon JP. Steroid receptor coactivator 2 is required for female fertility and mammary morphogenesis: insights from the mouse, relevance to the human. Nucl Recept Signal 2007; 5:e011.
19. Lee K, Jeong J, Kwak I, Yu CT, Lanske B, Soegiarto DW, Toftgard R, Tsai MJ, Tsai S, Lydon JP, DeMayo FJ. Indian hedgehog is a major mediator of progesterone signaling in the mouse uterus. Nat Genet 2006; 38:1204–1209.
20. Simmons DG, Rawn S, Davies A, Hughes M, Cross JC. Spatial and temporal expression of the 23 murine Prolactin/Placental Lactogen-related genes is not associated with their position in the locus. BMC Genomics 2008; 9:352.
21. Duggavathi R, Volle DH, Mataki C, Antal MC, Messaddeq N, Auwerx J, Murphy BD, Schoonjans K. Liver receptor homolog 1 is essential for ovulation. Genes Dev 2008; 22:1871–1876.
22. Challis JR, Lye SJ, Gibb W. Prostaglandins and parturition. Ann N Y Acad Sci 1997; 828:254–267.
23. Zakar T, Hertelendy F. Progesterone withdrawal: key to parturition. Am J Obstet Gynecol 2007; 196:289–296.
24. Conlon FL, Lyons KM, Takaesu N, Barth KS, Kispert A, Herrmann B, Robertson EJ. A primary requirement for nodal in the formation and maintenance of the primitive streak in the mouse. Development 1994; 120: 1919–1928.
25. Lowe LA, Yamada S, Kuehn MR. Genetic dissection of nodal function in patterning the mouse embryo. Development 2001; 128:1831–1843.
26. Ma GT, Soloveva V, Tzeng SJ, Lowe LA, Pfendler KC, Iannaccone PM, Kuehn MR, Linzer DI. Nodal regulates trophoblast differentiation and placental development. Dev Biol 2001; 236:124–135.
27. Guzman-Ayala M, Ben-Haim N, Beck S, Constam DB. Nodal protein processing and fibroblast growth factor 4 synergize to maintain a trophoblast stem cell microenvironment. Proc Natl Acad Sci U S A 2004; 101:15656–15660.
28. Natale DR, Hemberger M, Hughes M, Cross JC. Activin promotes differentiation of cultured mouse trophoblast stem cells towards a labyrinth cell fate. Dev Biol 2009; 335:120–131.
29. Munir S, Xu G, Wu Y, Yang B, Lala PK, Peng C. Nodal and ALK7 inhibit proliferation and induce apoptosis in human trophoblast cells. J Biol Chem 2004; 279:31277–31286.
30. Xu G, Zhong Y, Munir S, Yang BB, Tsang BK, Peng C. Nodal induces apoptosis and inhibits proliferation in human epithelial ovarian cancer cells via activin receptor-like kinase 7. J Clin Endocrinol Metab 2004; 89: 5523–5534.
31. Wang H, Tsang BK. Nodal signalling and apoptosis. Reproduction 2007; 133:847–853.
32. Postovit LM, Margaryan NV, Seftor EA, Kirschmann DA, Lipavsky A, Wheaton WW, Abbott DE, Seftor RE, Hendrix MJ. Human embryonic stem cell microenvironment suppresses the tumorigenic phenotype of aggressive cancer cells. Proc Natl Acad Sci U S A 2008; 105:4329–4334.
33. Pfendler KC, Yoon J, Taborn GU, Kuehn MR, Iannaccone PM. Nodal and bone morphogenetic protein 5 interact in murine mesoderm formation and implantation. Genesis 2000; 28:1–14.
34. Jones RL, Kaitu'u-Lino TJ, Nie G, Sanchez-Partida LG, Findlay JK, Salamonsen LA. Complex expression patterns support potential roles for maternally derived activins in the establishment of pregnancy in mouse. Reproduction 2006; 132:799–810.
35. Adamson SL, Lu Y, Whiteley KJ, Holmyard D, Hemberger M, Pfarrer C, Cross JC. Interactions between trophoblast cells and the maternal and fetal circulation in the mouse placenta. Dev Biol 2002; 250:358–373.
36. Agostinis C, Bulla R, Tripodo C, Gismondi A, Stabile H, Bossi F, Guarnotta C, Garlanda C, De Seta F, Spessotto P, Santoni A, Ghebrehiwet B, et al. An alternative role of C1q in cell migration and tissue remodeling: contribution to trophoblast invasion and placental development. J Immunol 2010; 185:4420–4429.
37. Gewolb IH, Merdian W, Warshaw JB, Enders AC. Fine structural abnormalities of the placenta in diabetic rats. Diabetes 1986; 35: 1254–1261.
38. Burrows TD, King A, Loke YW. Trophoblast migration during human placental implantation. Hum Reprod Update 1996; 2:307–321.
39. Burton GJ, Woods AW, Jauniaux E, Kingdom JC. Rheological and physiological consequences of conversion of the maternal spiral arteries for uteroplacental blood flow during human pregnancy. Placenta 2009; 30: 473–482.
40. Cross JC, Hemberger M, Lu Y, Nozaki T, Whiteley K, Masutani M, Adamson SL. Trophoblast functions, angiogenesis and remodeling of the maternal vasculature in the placenta. Mol Cell Endocrinol 2002; 187: 207–212.
41. Roberts DJ, Post MD. The placenta in pre-eclampsia and intrauterine growth restriction. J Clin Pathol 2008; 61:1254–1260.
42. Nadeem L, Munir S, Fu G, Dunk C, Baczyk D, Caniggia I, Lye S, Peng C. Nodal signals through activin receptor-like kinase 7 to inhibit trophoblast migration and invasion: implication in the pathogenesis of preeclampsia. Am J Pathol 2011; 178:1177–1189.
43. Hirota Y, Daikoku T, Tranguch S, Xie H, Bradshaw HB, Dey SK. Uterine-specific p53 deficiency confers premature uterine senescence and promotes preterm birth in mice. J Clin Invest 2010; 120:803–815.
44. Iguchi T, Tani N, Sato T, Fukatsu N, Ohta Y. Developmental changes in mouse placental cells from several stages of pregnancy in vivo and in vitro. Biol Reprod 1993; 48:188–196.
45. Ogle TF, Dai D, George P, Mahesh VB. Stromal cell progesterone and estrogen receptors during proliferation and regression of the decidua basalis in the pregnant rat. Biol Reprod 1997; 57:495–506.
46. Han YW, Redline RW, Li M, Yin L, Hill GB, McCormick TS. Fusobacterium nucleatum induces premature and term stillbirths in pregnant mice: implication of oral bacteria in preterm birth. Infect Immun 2004; 72:2272–2279.
47. Faye-Petersen OM. The placenta in preterm birth. J Clin Pathol 2008; 61: 1261–1275.